ARTICLE

Supporting Information

Patterned flexible graphene sensor via printing and interface assembly

Tangyue Xue,[a, c] Huige Yang,[a] Bin Shen,[b] Fengyu Li,*[b] Meng Su,[c] Xiaotian Hu,[c] Wentao Liu[a] and Yanlin Song*[c]

T. Y. Xue, Dr. H. G. Yang, Prof. W. T. Liu
School of Materials Science and Engineering, Zhengzhou University, Zhengzhou 450001, China.
B. Shen, Prof. F. Y. Li
College of Chemistry and Materials Science, Jinan University, Guangzhou 510632, China
*E-mail: lifengyu@jnu.edu.cn
Dr. M. Su, X. Hu, Prof. Y. L. Song
Key Laboratory of Green Printing, CAS Research/Education Center for Excellence in Molecular Sciences, Institute of Chemistry, Chinese Academy of Sciences (ICCAS), Beijing Engineering Research Center of Nanomaterials for Green Printing Technology, National Laboratory for Molecular Sciences (BNLMS), Beijing 100190, P. R. China
*E-mail: ylsong@iccas.ac.cn

Supplementary Materials:
Supplementary Figure 1-11
Supplementary Table 1-3
References 1-4

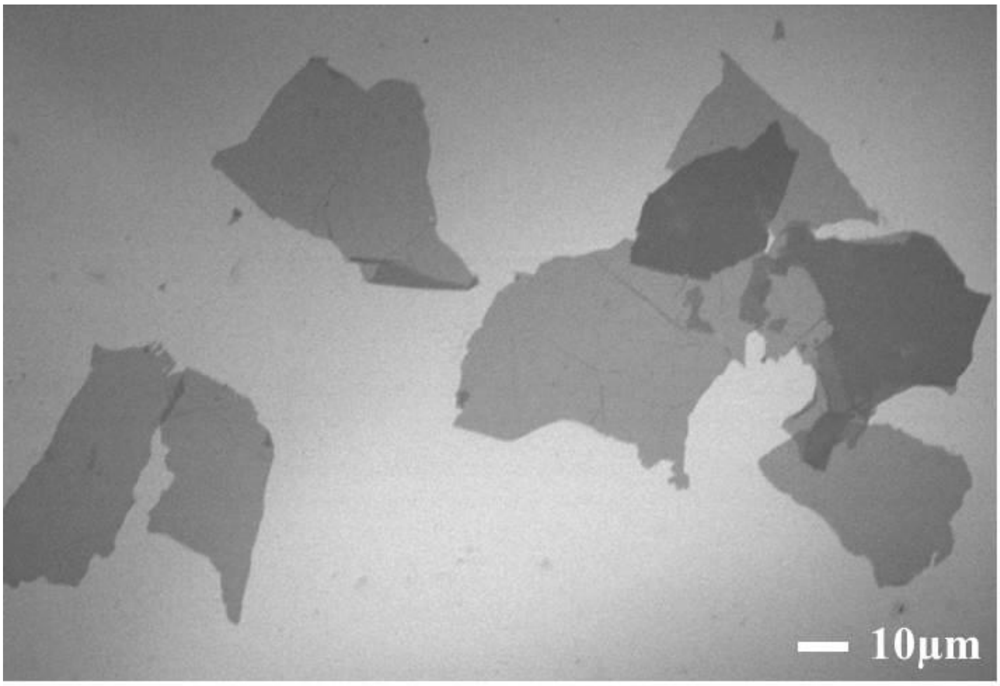

Fig. S1 The SEM image of GO. The lateral sizes of GO sheets distribute from 20 μm to 40 μm

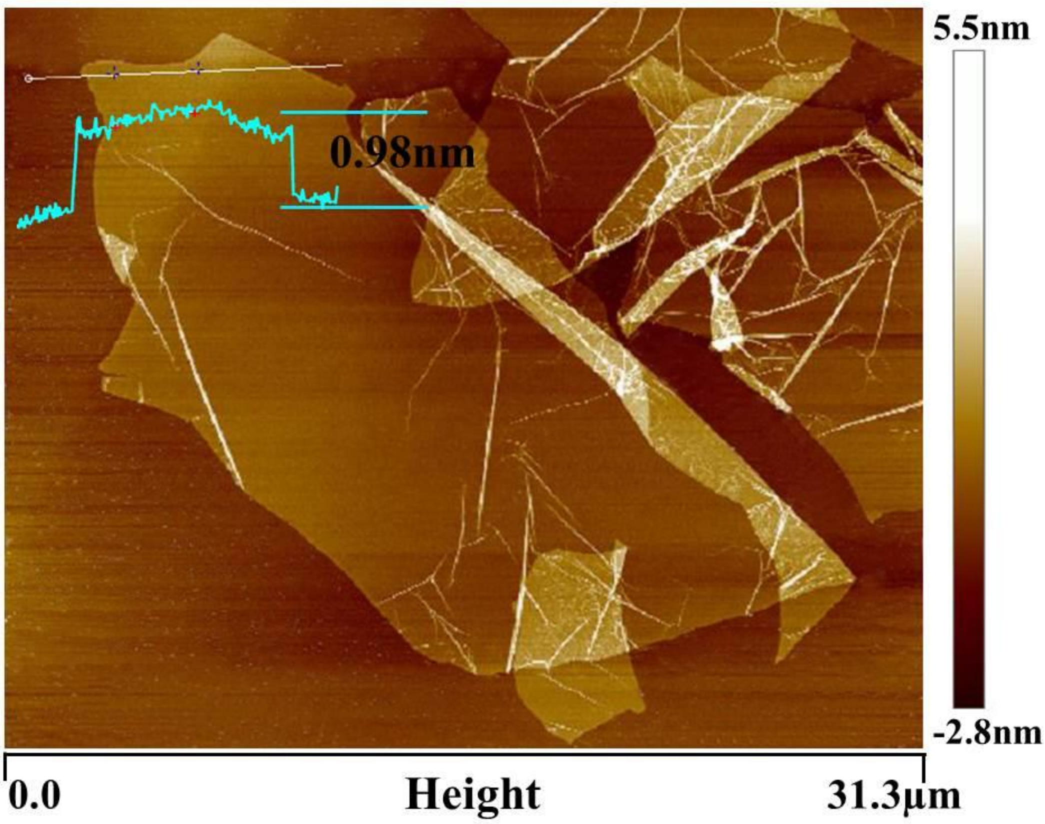

Fig. S2 The AFM image of GO. The typical thickness is characterized as 0.98 nm.

Please do not adjust margins

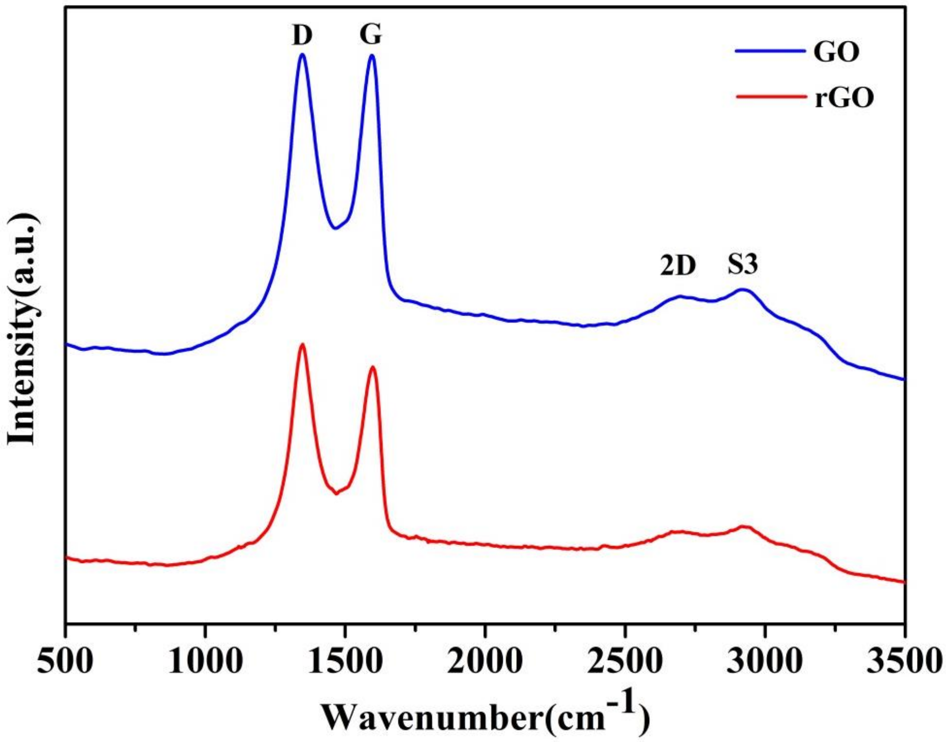

Fig. S3 The Raman spectra of the GO and rGO. The increase of I_D/I_G ratio reveals the partial restoration of C sp^2 in the rGO. The increase of the I_{2D}/I_{S3} ratio further indicates restoration of the conjugation structure after reduction.

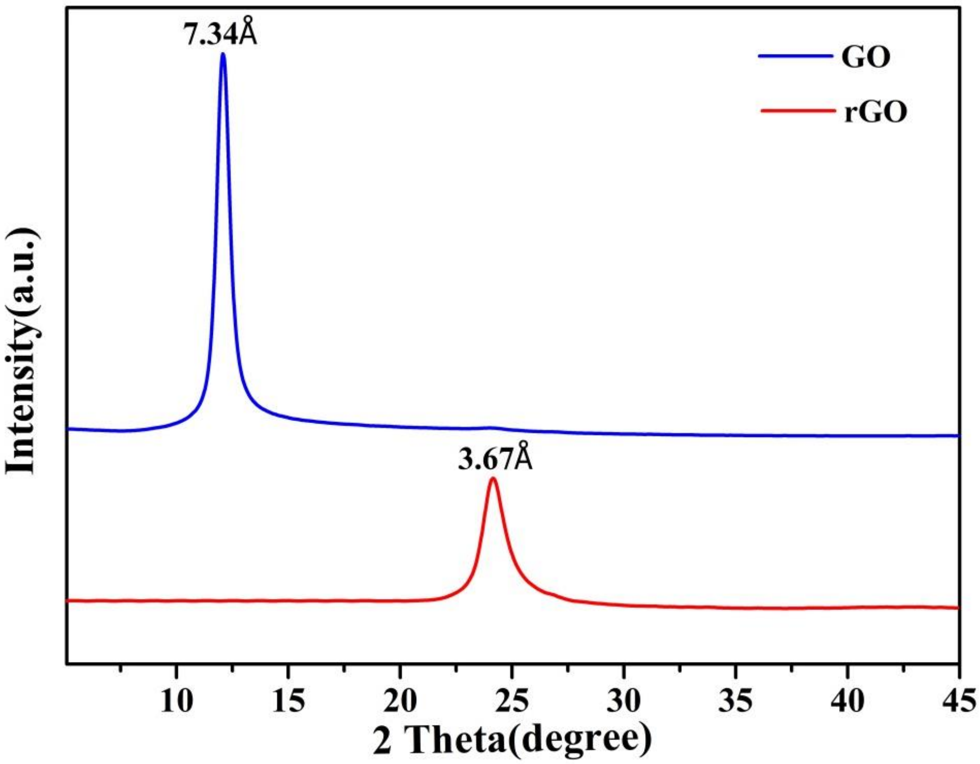

Fig. S4 The XRD patterns of the GO and rGO. The d spacing of GO and rGO are 7.34 Å and 3.67 Å, respectively. The decreasing interlamellar spacing is due to partial removal of the oxygen-containing groups after reduction.

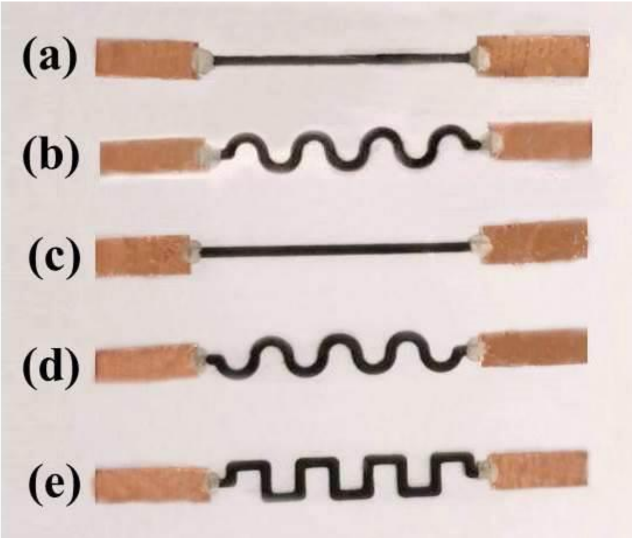

Fig. S5 The photographs showing (a) linear ribbon (b) wavy ribbon (c) linear aerogel (d) wavy aerogel (e) serpentine aerogel of printed graphene sensors.

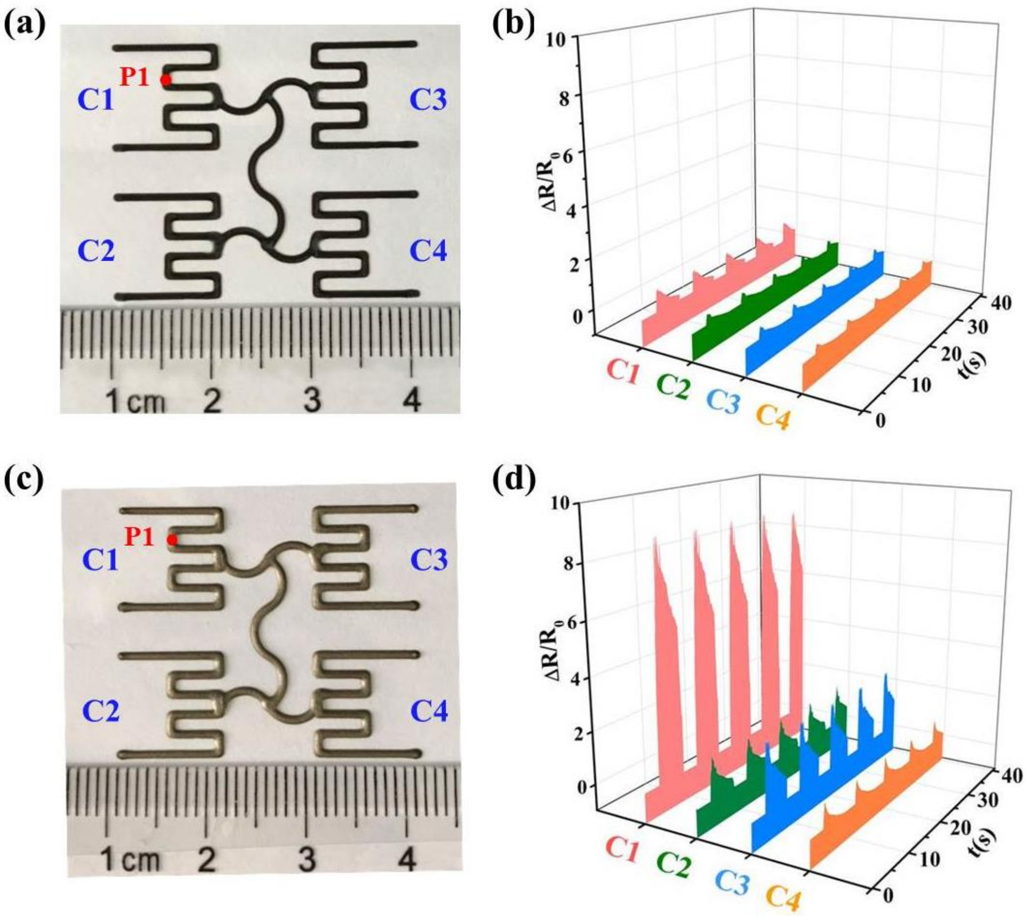

Fig. S6 The optical images and the real-time resistance monitoring of the integrated patterned graphene sensors with different microstructures graphene ribbon and graphene aerogel: (a) the optical images and (b) the relative resistance changes ($\Delta R/R_0$) of 4 channels of the patterned graphene ribbon sensor when applying force to point P1, where P1 is the force point and C1-C4 is the 4 channels of the sensor; (c) the optical images and (d) the relative resistance changes ($\Delta R/R_0$) of 4 channels of the patterned graphene aerogel sensor when applying force to point P1.

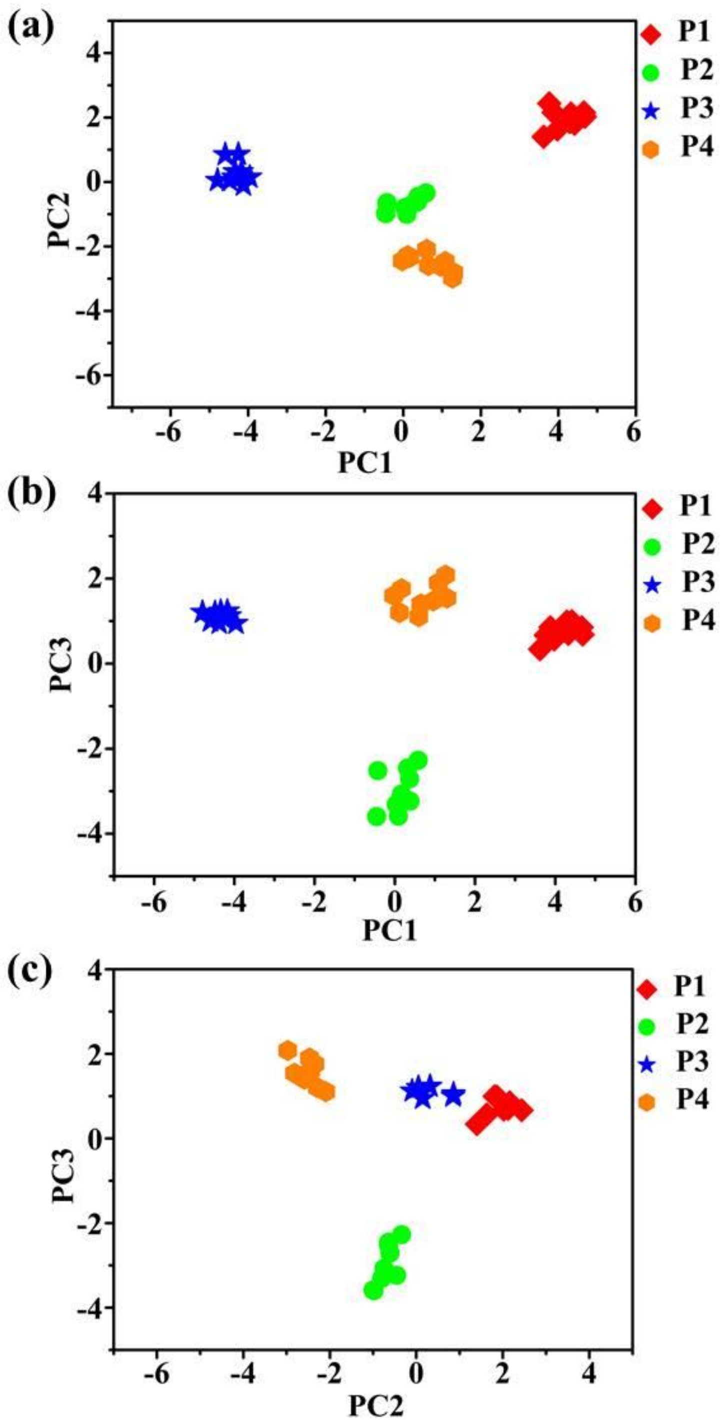

Fig. S7 The PCA score plots of the first three principal components of statistical significance for the four points of different orientations at the same position (P1-P4). (a), (b), (c) represent the PCA results at different projection, respectively.

Please do not adjust margins

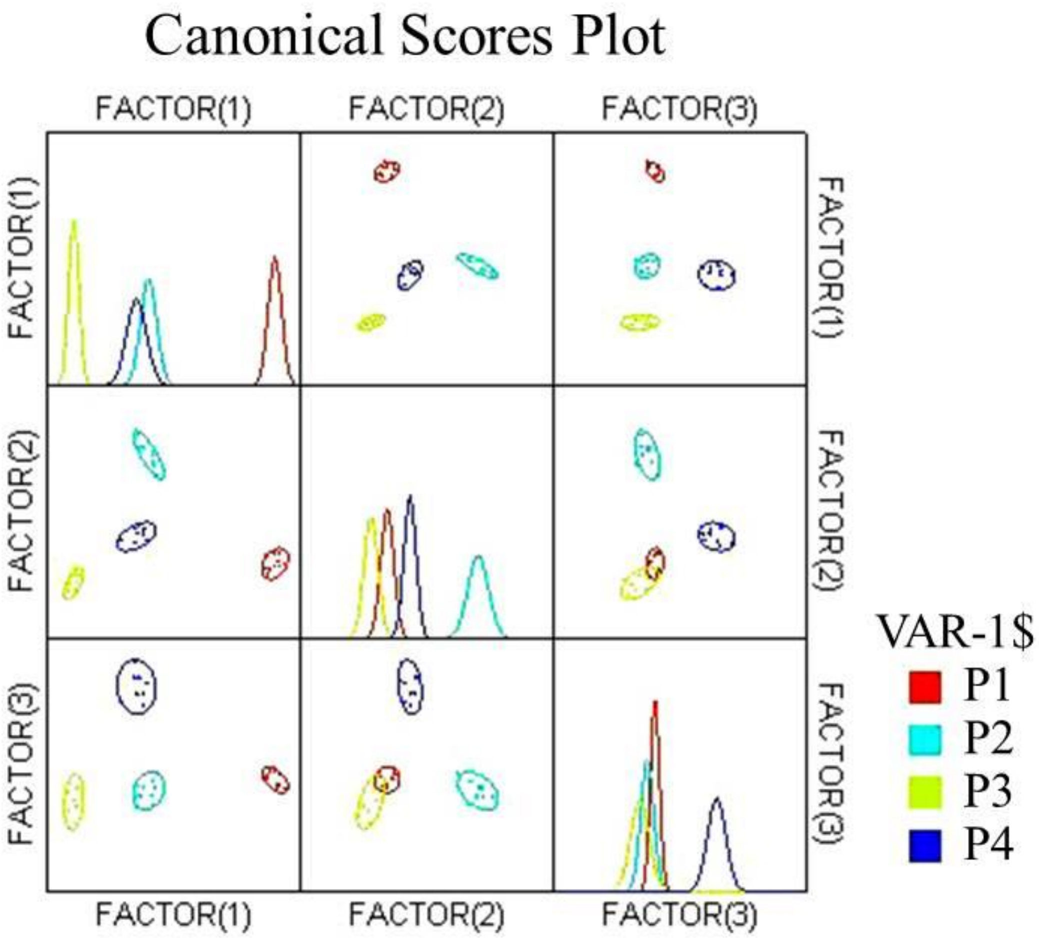

Fig. S8 The canonical scores plot of integrated flexible sensors for the discrimination of 4 differenet orientation and distance points(P1-P4).

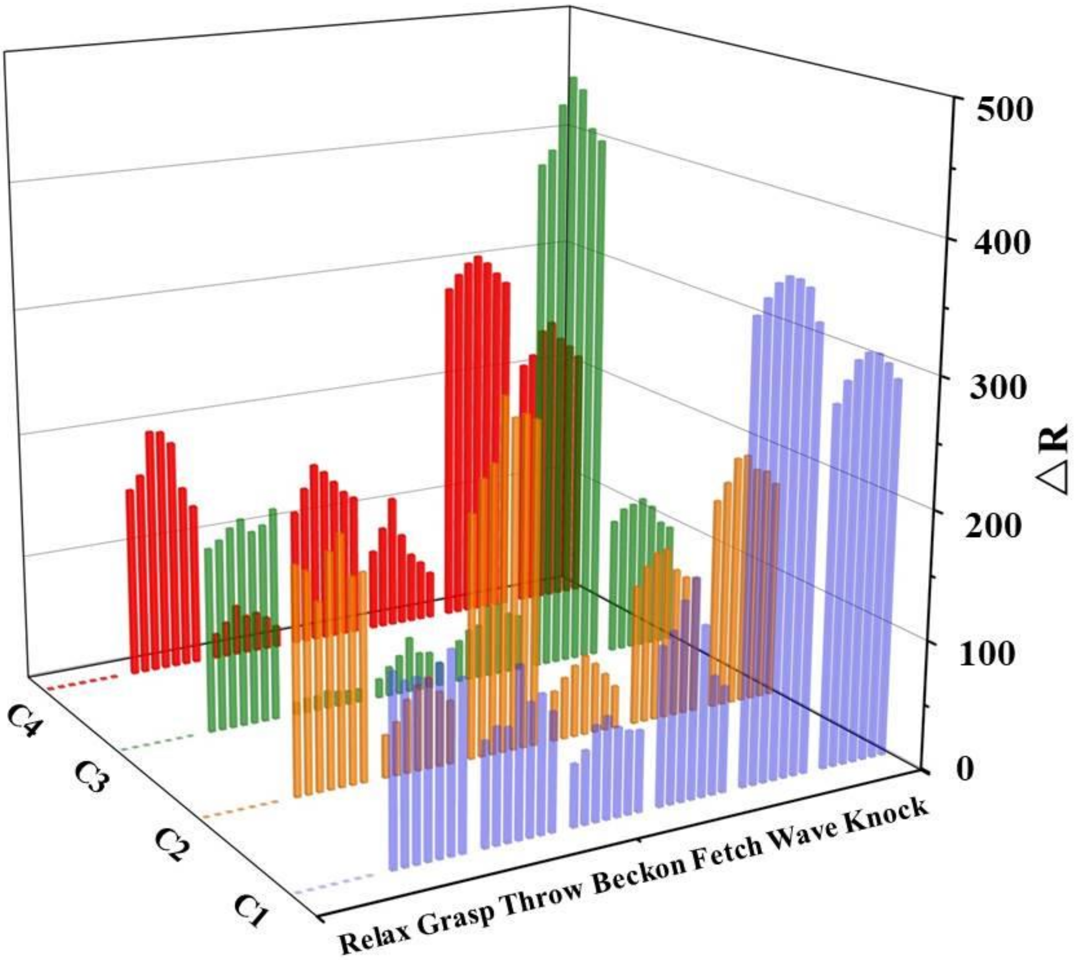

Fig. S9 The 3D chart display resistance changes of 7 different motion gestures which were monitored at human wrist with electronics data logger. Seven characteristic vales were readout at the peak or nadir of the monitoring resistance curves. There were 28 variables for each gesture to describe the detail movement responses.

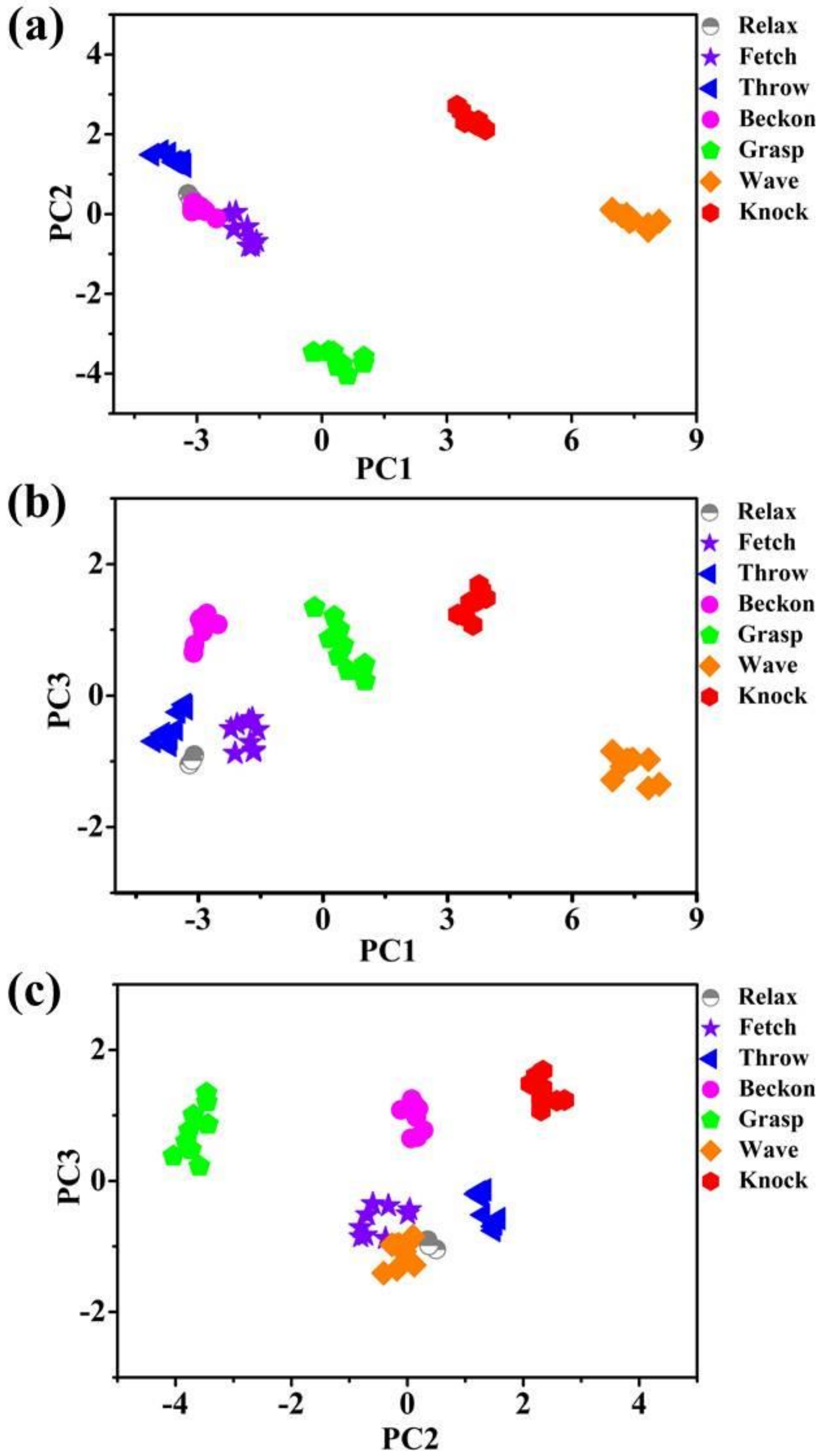

Fig. S10 The PCA score plots of the first three principal components of statistical significance for seven different wrist bending gestures. (a), (b), (c) represent the PCA results at different projection respectively.

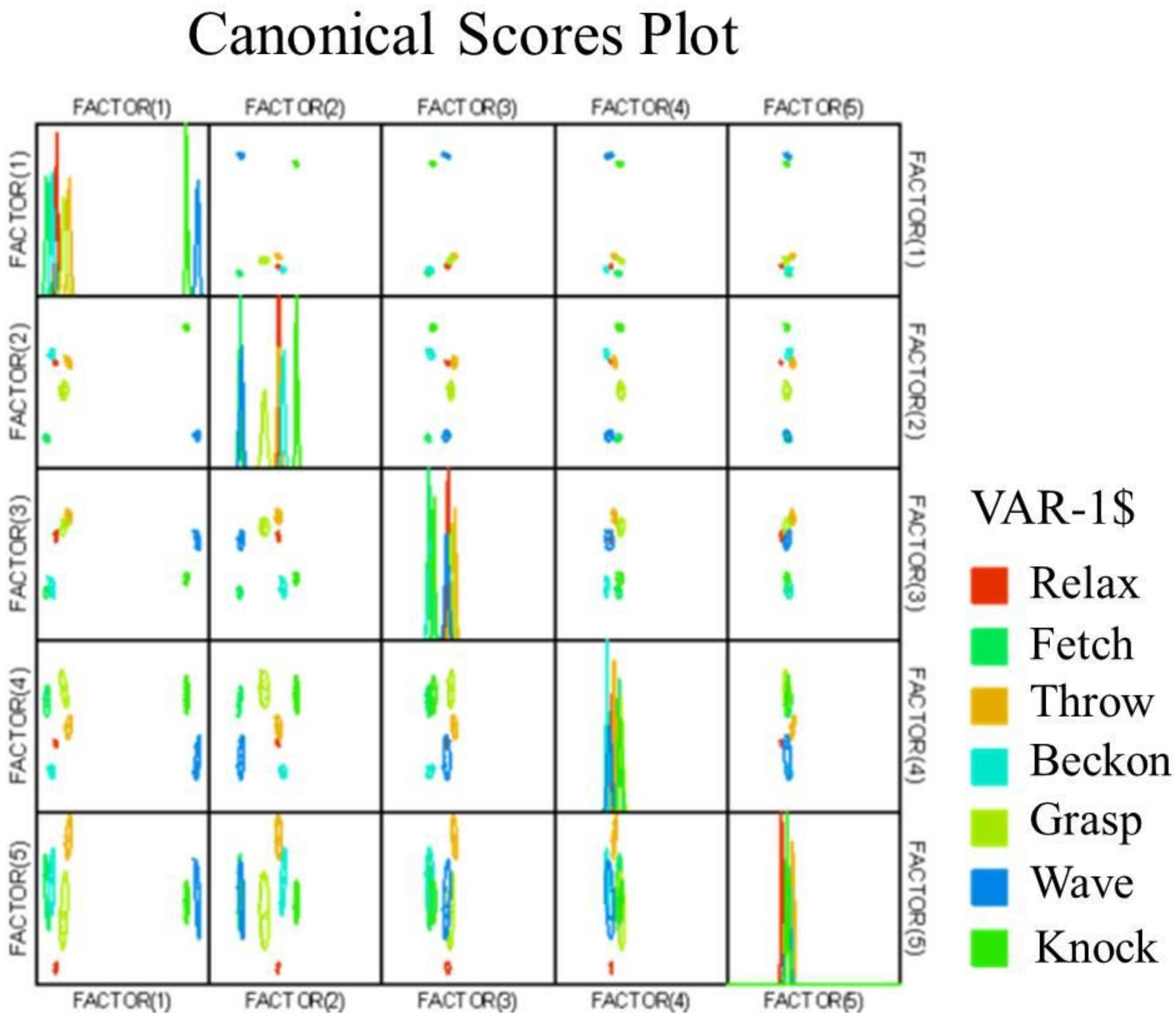

Fig. S11 The canonical scores plot of integrated flexible sensors for the discrimination of seven different wrist gestures.

Table S1. Comparison of Performance Parameters for Different Graphene-based Strain Sensors

Graphene-based strain sensor	Preparation methods	Strain range	Gauge factor	Electrical conductivity (S/m)	Ref.
Graphene woven microfabrics	CVD	0-8%	500(0-2%) 10^4(2%-8%)	-	[1]
Nanographene film	Exfoliation graphene infusion into the rubber	0.5-1.6%	10-1000	0.1	[S1]
Ag-NPs/GO composite	Drop-casting	0-14.5%	475	-	[S2]
Graphene-fiber composites	UV lithography	0-100%	10(0-1%) 3.7(0-50%)	-	[S3]
Laser-scribed graphene	Laser direct writing	0-10%	9.49	-	[S4]
Graphene-based fiber	Modified Hummers; thermal reduction RGO(unannealed) Thermal annealed RGO(1200°C) RGO@PDA(50%,unannealed) RGO@C(50%, 1200°C) RGO@C(20%, 1200°C) RGO@C(30%, 1200°C)	12.76±0.85 2.32±0.48 4.32±0.58 2.31±0.70 1.52±0.17 1.71±0.18	-	8×10^2 1.87×10^2 12.7×10^2 6.16×10^4 6.61×10^4 6.32×10^4	[17]
Grid-patterned graphene film	Computer numerical control milling process; layer by layer assembly The non-patterned sensor for 3 layers The grid-patterned sensor for 3 layers	10-60% 10-25%	8.97-173.91 301.61-29631	-	[32]
Graphene aerogel	Direct ink printing Linear aerogel	0-100%	5.2	GA:3.46×10^2	[33]
Graphene ribbon	Direct ink printing Linear ribbon	-	-	GR:4.51×10^4	[34]
Integration patterned graphene ribbon and graphene aerogel	Direct ink printing Linear ribbon Wavy ribbon Linear aerogel Wavy aerogel Seperntine aerogel	0-18% 0-27% 0-100% 0-100% 0-100%	0.03 0.29 4.81 6.55 8.89	GR:4.21×10^4 GA:3.23×10^2	This work

Table S2. The jackknifed classification procedure in four points (P1-P4) of integrated flexible sensors. Summary of 36 samples classification of four different orientation and distance points by linear discriminant analysis (LDA).

Jackknifed Classification Matrix on four points (P1-P4)					
	P1	P2	P3	P4	Correct
P1	9	0	0	0	100%
P2	0	8	0	1	89%
P3	0	0	9	0	100%
P4	0	0	0	9	100%
Total	9	8	9	10	97%
N = 36		N Correct = 35			Proportion Correct = 0.97

Table S3. The jackknifed classification procedure for wrist motion monitoring of integrated flexible sensors. Summary of 63 samples classification of one relax form (control) and six wrist movements data by linear discriminant analysis (LDA).

Jackknifed Classification Matrix at wrist motion monitoring								
	Relax (Control)	Fetch	Throw	Beckon	Grasp	Wave	Knock	Correct
Relax (Control)	9	0	0	0	0	0	0	100%
Fetch	0	9	0	0	0	0	0	100%
Throw	0	0	9	0	0	0	0	100%
Beckon	0	0	0	9	0	0	0	100%
Grasp	0	0	0	0	9	0	0	100%
Wave	0	0	0	0	0	9	0	100%
Knock	0	0	0	0	0	0	9	100%
Total	9	9	9	9	9	9	9	100%
N = 63					N Correct = 63			Proportion Correct = 1.000

References

[S1] J. Zhao, G. Wang, R. Yang, X. Lu, M. Cheng, C. He, G. Xie, J. Meng, D. Shi and G. Zhang, *ACS Nano*, 2015, **9**, 1622-1629.

[S2] Z. Yang, D. Y. Wang, Y. Pang, Y. X. Li, Q. Wang, T. Y. Zhang, J. B. Wang, X. Liu, Y. Y. Yang, J. M. Jian, M. Q. Jian, Y. Y. Zhang, Y. Yang and T. L. Ren, *ACS Appl. Mater. Interfaces*, 2018, **10**, 3948-3954.

[S3] Y. Cheng, R. Wang, J. Sun and L. Gao, *Adv. Mater.,* 2015, **27**, 7365-7371.

[S4] H. Tian, Y. Shu, Y. L. Cui, W. T. Mi, Y. Yang, D. Xie and T. Li. Ren, *Nanoscale*, 2014, **6**, 699-705.